Global Leaf Trait Relationships: Mass, Area, and the Leaf Economics Spectrum

Jeanne L. D. Osnas *et al.*

Science **340**, 741 (2013);
DOI: 10.1126/science.1231574

Global Leaf Trait Relationships: Mass, Area, and the Leaf Economics Spectrum

Jeanne L. D. Osnas,[1,2]* Jeremy W. Lichstein,[2] Peter B. Reich,[3,4] Stephen W. Pacala[1]

The leaf economics spectrum (LES) describes multivariate correlations that constrain leaf traits of plant species primarily to a single axis of variation if data are normalized by leaf mass. We show that these traits are approximately distributed proportional to leaf area instead of mass, as expected for a light- and carbon dioxide–collecting organ. Much of the structure in the mass-normalized LES results from normalizing area-proportional traits by mass. Mass normalization induces strong correlations among area-proportional traits because of large variation among species in leaf mass per area (LMA). The high LMA variance likely reflects its functional relationship with leaf life span. A LES that is independent of mass- or area-normalization and LMA reveals physiological relationships that are inconsistent with those in global vegetation models designed to address climate change.

Leaf size varies by several orders of magnitude between species, and leaf traits are typically normalized by mass or area to study relationships among them. The leaf economics spectrum (LES) (*1*, *2*) has received considerable attention in part because the tight relationships among mass-normalized leaf traits appear to constrain the biodiversity of leaves to a single axis (Fig. 1). The apparent simplicity of this relationship is appealing because of the need to summarize functionally important aspects of biodiversity in models of the terrestrial carbon cycle and climate change (*3*–*6*).

The GLOPNET (Global Plant Trait Network) leaf traits data set (*2*), from which the LES was generated, reports values of maximum rate of net photosynthesis (A_{max}), dark respiration rate (R_{dark}), nitrogen (N) and phosphorus (P), leaf life span (LL), and leaf mass per area (LMA, which increases with leaf thickness and tissue density) (throughout this paper, we use "N" and "P" to refer to concentrations per unit leaf area or mass, and we use the words "nitrogen" and "phosphorus" to refer generically to the elements). Correlations among traits in GLOPNET [primarily reflecting interspecific variation (*7*)] are much

[1]Department of Ecology and Evolutionary Biology, 106 Guyot Hall, Princeton University, Princeton, NJ 08542, USA. [2]Department of Biology, University of Florida, 317 Carr Hall, Gainesville, FL 32611, USA. [3]Department of Forest Resources, University of Minnesota, 115 Green Hall, 1530 Cleveland Avenue North, St. Paul, MN 55108, USA. [4]Hawkesbury Institute for the Environment, University of Western Sydney, Locked Bag 1797, Penrith, NSW 2751, Australia.

*Corresponding author. E-mail: jldosnas@gmail.com

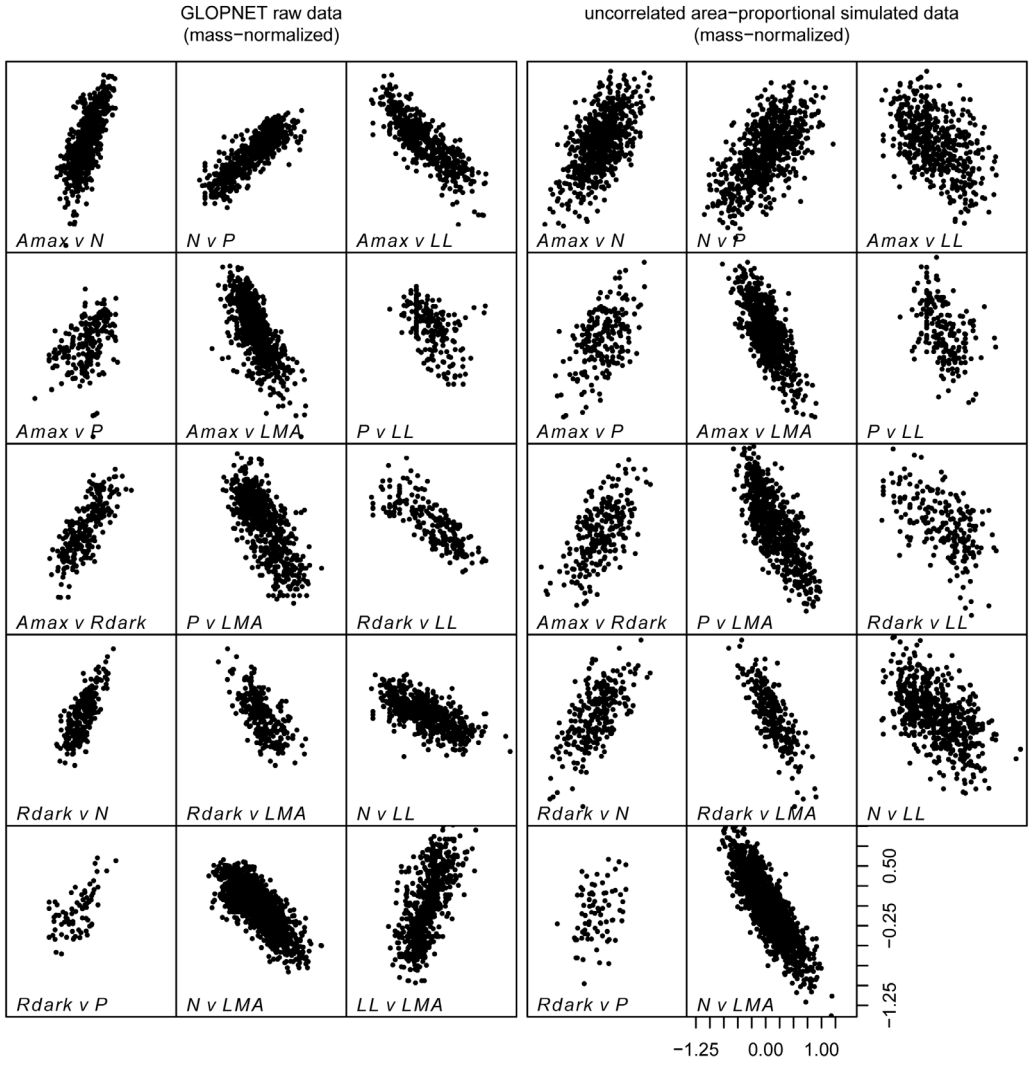

Fig. 1. Observed mass-normalized LES (left three columns) and mass-normalized predictions from an area-proportional null model with no functional correlations involving A_{max}, R_{dark}, N, or P (right three columns). The observed mass-normalized LES and the null model (which leaves intact the actual LMA-LL relationship) have similar overall structure but differ quantitatively due to relationships not caused by mass normalization. All values are $\log_{10}$-transformed with means rescaled to (0,0).

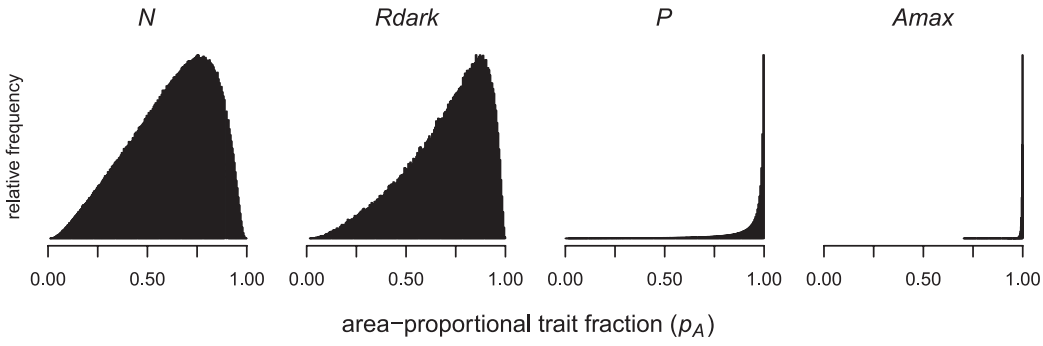

Fig. 2. Frequency of species with area-proportional trait fraction p_A and mass-proportional fraction $1 - p_A$ for N, R_{dark}, P and A_{max} in GLOPNET. A p_A value of 1 indicates pure area proportionality, whereas 0 indicates pure mass proportionality. The histograms are estimated from the posterior distribution of parameters from Model-C and account for parameter uncertainty and the distribution of LMA values in GLOPNET (*7*). All four traits (especially A_{max} and P) are primarily area proportional for most species.

stronger if A_{max}, R_{dark}, N, and P are normalized by mass than if normalized by area (Fig. 1 and fig. S1).

By definition, a trait is distributed proportional to mass if normalizing by mass makes the trait statistically independent of mass, area, and LMA (*7*). Similarly, area normalization removes all effects of leaf size from an area-proportional trait. If a trait is mass-proportional, then the total (non-normalized) trait amount in leaves of species with the same leaf mass does not increase with leaf area (i.e., the trait does not vary with LMA among species that share the same leaf mass), whereas if a trait is area-proportional, it does not increase with leaf mass among species with the same area. We statistically partitioned A_{max}, R_{dark}, N and P in GLOPNET into area- and mass-proportional components (Fig. 2) (*7*). Almost all A_{max} and P are proportional to area in nearly all species, and most leaf N and R_{dark} are area-proportional in more than 90% of species (Fig. 2) (*7*). If mass- and area-proportionality hypotheses are given equal prior probabilities, then the posterior probability of the former is less than 10^{-25} for each of the four traits (*7*).

The possibility that the strong correlations among per-unit-mass traits are largely the result of mass normalization of area-proportional traits was discussed in qualitative terms by Field and Mooney (*8*, *9*). This alert has gone largely unnoticed in subsequent studies of leaf traits, perhaps because quantitative estimates of mass versus area proportionality were unavailable until now (Fig. 2). Mass normalization of area-proportional traits induces positive covariance between these traits and negative covariance between each of them and LMA by an amount equal to the variance of LMA [using log-transformed data (*7*)], which is large in GLOPNET (LMA range: 14 to 1509 g m^{-2}). Thus, much of the structure of the mass-based GLOPNET LES is a direct joint result of (i) traits being primarily area-proportional and (ii) high LMA variance, which is a result of the global LL-LMA tradeoff. LL is neither area- nor mass-based, so the strong LL-LMA correlation reported in (*1*, *2*) is unaffected by normalization and likely indicates a robust relationship. The high LMA of long-lived leaves may be necessary to provide the structure and defense needed for long life, which increases nutrient-use efficiency (*1*, *2*, *10*–*12*). Also, because high-LMA leaves are expensive to produce (per unit area) and have similar mean A_{max} per area as low-LMA leaves (*1*), these high-LMA leaves must live a long time if they are to pay back their construction costs (*2*, *10*). The tradeoff between fast returns on construction costs (low LMA) and long-term returns combined with high nutrient-use efficiency (high LL) likely contributes to the interspecific covariation between LMA and LL (*1*, *2*). Unlike the LL-LMA relationship, most of the covariance between mass-based traits and LL in GLOPNET is due to mass normalization of primarily area-proportional traits that are only weakly correlated with LL (*7*). The LMA-induced covariances in GLOPNET are quantitatively close to the actual covariances in the mass-normalized LES (Fig. 3), which illustrates the dominance of the covariances created by mass normalization.

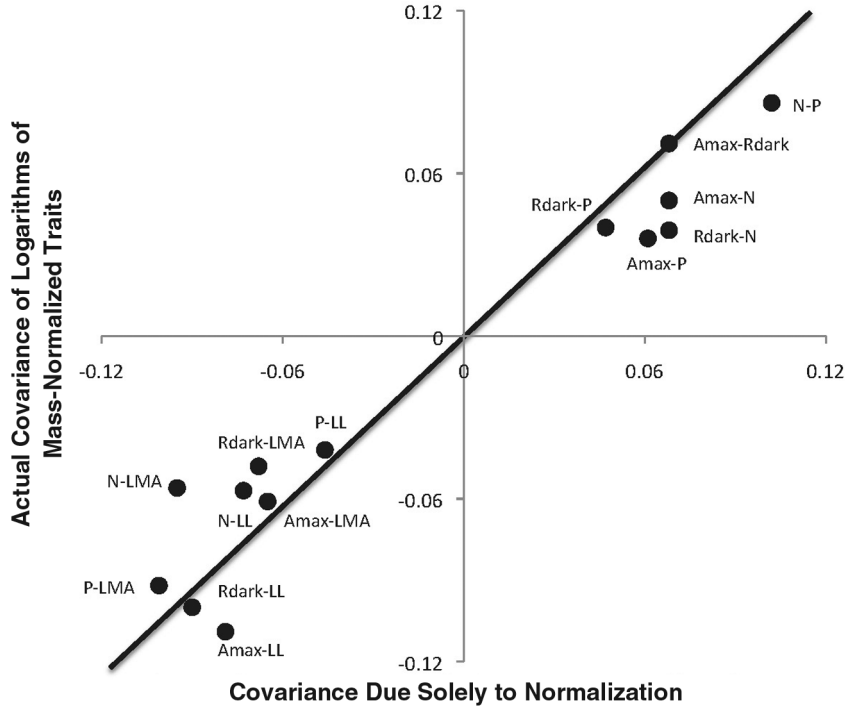

Fig. 3. Actual covariances between logarithms of mass-normalized traits in GLOPNET versus those induced by mass normalization of area-proportional traits. If A_{max}, R_{dark}, N, and P were distributed across species purely proportional to area, then mass normalization would induce the following covariances: $-VAR(\log_{10}LMA)$ for comparisons involving LMA, $-COV(\log_{10}LL, \log_{10}LMA)$ for comparisons involving LL, and $VAR(\log_{10}LMA)$ for all others (*7*), where COV is covariance and VAR is variance. Values of $VAR(\log_{10}LMA)$ and $COV(\log_{10}LL, \log_{10}LMA)$ differ for each combination of traits because not all trait values are reported for every species in GLOPNET. Departures of the actual covariances from those predicted to occur solely because of mass normalization are caused by covariances among the minor mass-distributed trait fractions (Fig. 2) and by normalization-independent correlations (figs. S4 and S5).

To further illustrate the effects of mass normalization, we generated random area-proportional values for A_{max}, R_{dark}, N, and P from statistically independent log-normal distributions with the

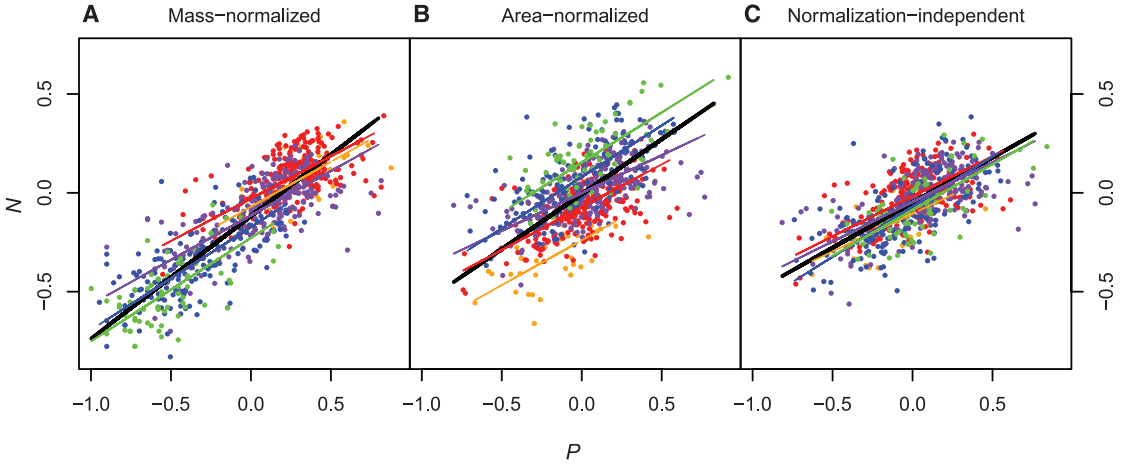

Fig. 4. Scatter plots of N versus P from GLOPNET. (**A**) Mass-normalized data. (**B**) Area-normalized data. (**C**) Normalization-independent values (residuals from Eqs. 1 and 2). Values are $\log_{10}$-transformed with means rescaled to zero and colored by the $\log_{10}$LMA *z* score (number of standard deviations from mean $\log_{10}$LMA): $z \leq -1$, orange; $-1 < z \leq 0$, red; $0 < z \leq 1$, violet; $1 < z \leq 2$, blue; and $2 < z$, green. Lines show major axis regressions (black, full data set; colored, LMA bins). Slopes of colored lines are not significantly different from each other or from the black line in (C), but they are significantly different from slopes of black lines in (A) and (B) (*7*), indicating that the normalization-independent LES is approximately equivalent to sorting species by LMA.

same means and variances as the area-normalized GLOPNET data. We then mass-normalized these random values by dividing them by randomly chosen GLOPNET LMA values (Fig. 1). All correlations in the right-hand panels of Fig. 1 are caused solely by mass normalization and simply reflect the correlation of LMA with either itself or LL. The random values reproduce the general structure in the mass-normalized LES (area-normalized counterpart in fig. S1), even though they lack any functional correlations among A_{max}, R_{dark}, N, and P, such as the physiological dependence of A_{max} on N (*2*, *6*, *8*, *9*, *13*). Discrepancies between the correlations, slopes, and intercepts of the mass-based LES and those generated from the random LES reflect trait relationships that are not induced by mass normalization and that represent the core of the normalization-independent LES discussed below. Area normalization of randomly generated mass-proportional values produces results unlike the data (fig. S3).

A simple hypothesis explains both the area proportionality of traits and the strong interspecific correlations in the mass-normalized LES in GLOPNET. Evolution has distributed traits associated with photosynthetic function primarily proportional to area, because all leaves are designed to intercept light and capture CO_2. Regardless of mesophyll depth, only a few cell layers of mesophyll are responsible for the bulk of light capture and photosynthesis (*11*, *13*, *16*, *17*). However, the large variation in LMA and the strong global LL-LMA relationship imply that plant species vary in their investment in nonphotosynthetic functions that increase longevity and require large LMA, such as structural rigidity and defense. Thus, area-normalized light interception, water loss, and photosynthetic traits vary much less than isometrically with LMA. Large variance in LMA reflects variation in ecological conditions that select for different optimal LLs. Together, these factors lead to nearly area-proportional A_{max}, R_{dark}, N, and P; large mass-normalized variance of these traits at any given leaf area; and thus, large correlations induced by mass normalization.

Dark respiration rate, N, and P are primarily proportional to area because their main function is to support photosynthesis. The significant but minor portion of R_{dark} that is distributed proportional to mass (Fig. 2) likely reflects interspecific variation in GLOPNET in the number and depth of respiring cell layers. The mass-distributed portion of N may be both structural and functional. Every cell wall in a leaf contains nitrogen in structural proteins. Some nitrogen may also contribute to nonphotosynthetic functions, such as carbohydrate dynamics and defense (*8*). The role of the mass-distributed portion of N and R_{dark} in structural rigidity and defense probably contributes to the strong relationship between LMA and LL. Phosphorus is located primarily in organelles in the cytosol (*14*) and is therefore not as closely bound to LMA as structural nitrogen. The stoichiometric ratio of N to P increases with LMA in GLOPNET (*12*) because, on average, mass-proportional fractions are larger for N than for P.

Because normalization-induced covariance scales with the variance of logLMA, it can be minimized by sorting species into groups with similar LMA. Doing so with GLOPNET reveals that area and mass normalization produce similar trait relationships, both within a given LMA group (compare the slopes of same-colored lines between Fig. 4, A and B) and between groups with different LMA (compare the slopes of lines with different colors within Fig. 4, A and B). The similarity of slopes across LMA groups reflects the approximate multivariate log-normality of the GLOPNET data and points to a new LES defined by the multivariate normal distribution of the logarithms of A_{max}, R_{dark}, N, and P conditional on log(LMA) (*7*). Previous analyses included LMA as a covariate when regressing one trait on another (*1*, *2*, *9*). Here, we extend this approach to derive a normalization-independent LES for A_{max}, R_{dark}, N, and P that is independent of LMA and mass or- area normalization (*7*). Consider the following ordinary least-squares (OLS) regressions

$$\log_{10}X_{Aik} = I_i + S_i \times \log_{10}\mathrm{LMA}_k + n_{ik} \quad (1)$$

$$\log_{10}X_{Mik} = I_i + (S_i - 1) \times \log_{10}\mathrm{LMA}_k + n_{ik} \quad (2)$$

where $\log_{10}X_{Aik}$ and $\log_{10}X_{Mik}$ are, respectively, $\log_{10}$-transformed area- and mass-normalized values for trait *i*, species *k*; I_i and S_i are intercept and slope parameters for trait *i*; and n_{ik} is a normally distributed residual. Subtracting $\log_{10}\mathrm{LMA}_k$ from both sides of Eq. 1 yields Eq. 2. Thus, Eqs. 1 and 2 are mathematically identical: Both regressions yield identical estimates for I_i and S_i and identical values for n_{ik}. Plotting the residuals for two traits against each other shows the normalization-independent relationships (Fig. 4C), which are very similar to those obtained from sorting species into LMA groups (Fig. 4, A and B). Estimates of S_i are consistent with the independently estimated area- versus mass-proportional fractions in Fig. 2 (see comparison in fig. S6), which suggests that the normalization-independent LES accurately captures functional relationships between traits that are altered by area and (especially) mass normalization.

The normalization-independent LES probably reflects universal functional constraints and/or adaptation affecting leaf carbon and nutrient dynamics (*2*, *11*, *15*). Pairwise and multivariate trait relationships estimated from the normalization-independent values (i.e., residuals from Eqs. 1 and 2) are usually intermediate in strength between those estimated from area- and mass-normalized values and sometimes have significantly different regression slopes. For example [see also (*7*)], the standardized major axis regression slope [commonly used in allometry (*12*)] between mass-normalized N and P in GLOPNET is 0.67, as predicted by metabolic scaling theory (*15*). However, 2/3 is significantly steeper than the normalization-independent slope of 0.59 (table S2) (*7*), implying that across the global flora, leaves accrue less N per unit P than predicted by metabolic theory.

The normalization-independent LES has important implications for global vegetation models (*5*, *6*), which include coupled carbon-nitrogen cycles but lack explicit treatment of biodiversity within a small number (roughly 10) of plant functional types (PFTs). Most of these models assume that A_{max} and R_{dark} are proportional to leaf nitrogen, which appears justified within the vertical canopy gradient of individual plants (*5*, *13*, *16*–*18*). However, much variation in N is the result of differences among species, and less than half of this interspecific variation is explained by global PFT classifications [see figure 5 in (*19*)]. The assumption that A_{max} and R_{dark} are proportional to N (log-log slopes of 1) appears reasonably consistent with the log-log OLS slopes of per-unit-mass A_{max} and R_{dark} versus N (1.25 ± 0.04 and 1.06 ± 0.06, respectively; OLS regression because changes in N are assumed causal), but these slopes are amplified by hidden changes in LMA (*7*). If a high-N species replaces a low-N species with the same LMA, then the correct dependencies of A_{max} and R_{dark} on N are given by the normalization-independent OLS slopes (0.68 ± 0.05 for A_{max} versus N; 0.66 ± 0.0 for R_{dark} versus N), which control for LMA. The slopes obtained from mass-normalized traits are too steep, implying a carbon-nitrogen feedback that is too strong. In contrast, the carbon-cycle feedback implied by area-based OLS slopes is too weak (0.45 ± 0.04 for A_{max} versus N; 0.65 ± 0.06 for R_{dark} versus N) because N per area (but not A_{max} per area) increases with LMA due to its substantial mass-proportional fraction (Fig. 2); this inflates the variance in the independent variable (N) in the regression and reduces the estimated slope (*7*).

The preceding example assumes that species replacement is associated with increasing N but constant LMA. Because LMA may also change, we now consider the opposite extreme, in which normalization-independent N is held constant and LMA is variable, so that per area increases as LMA increases. In this case, interspecific patterns in GLOPNET imply that an increase in N per area (holding normalization-independent N constant) would be associated with almost no change in A_{max} and a weak increase in R_{dark} (log-log slopes of A_{max} per area and R_{dark} per area on N per area, conditional on constant normalization-independent N: 0.06 ± 0.04 and 0.50 ± 0.07, respectively). Thus, the A_{max}-N and R_{dark}-N relationships in many global models are again steeper than the interspecific patterns in GLOPNET. Because R_{dark} per area increases more quickly with N per area than A_{max} per area, net carbon gain per unit leaf area may actually decrease as N per area increases. Intermediate cases involving changes in both LMA and normalization-independent N produce leaf-level A_{max}-N and R_{dark}-N dependencies that are intermediate between the two extreme cases.

Inconsistencies between the interspecific trait relationships in GLOPNET and the relationships in global vegetation models, and the large amount of within-PFT trait variation in nature (*19*), imply that global models will need more realistic treatments of biodiversity if they are to predict global carbon-nitrogen feedbacks. Greater biodiversity could be included in global models by replacing discrete PFTs with a species continuum (*2*). On the surface, the 15 tight correlations of the mass-normalized LES appear to offer the possibility of capturing 75% of global leaf trait diversity with a single principal component axis (*2*). However, because much of this visually appealing structure is the result of normalization combined with LMA variation, this single axis excludes important aspects of biodiversity that are orthogonal to LMA. Accurately representing biodiversity in global models will probably require including at least two axes of variation, such as LMA and the first principal component of the normalization-independent LES (*7*). Alternatively, this normalization-independent axis could be used to represent interspecific variation within the PFTs currently used in global models.

References and Notes

1. P. B. Reich, M. B. Walters, D. S. Ellsworth, *Proc. Natl. Acad. Sci. U.S.A.* **94**, 13730 (1997).
2. I. J. Wright *et al.*, *Nature* **428**, 821 (2004).
3. G. B. Bonan, S. Levis, L. Kergoat, K. W. Oleson, *Global Biogeochem. Cycles* **16**, 5-1 (2002).
4. G. C. Hurtt *et al.*, *Proc. Natl. Acad. Sci. U.S.A.* **99**, 1389 (2002).
5. P. E. Thornton, N. E. Zimmermann, *J. Clim.* **20**, 3902 (2007).
6. S. Zaehle, A. D. Friend, *Global Biogeochem. Cycles* **24**, (2010).
7. See the materials and methods, as well as other supplementary materials on *Science* Online.
8. C. Field, H. Mooney, in *On the Economy of Plant Form and Function: Proceedings of the Sixth Maria Moors Cabot Symposium, Evolutionary Constraints on Primary Productivity, Adaptive Patterns of Energy Capture in Plants, Harvard Forest, August 1983*, T. J. Givnish, Ed. (Cambridge Univ. Press, New York, 1986), pp. 25–55.
9. C. Field, H. A. Mooney, *Oecologia* **56**, 348 (1983).
10. D. S. Falster *et al.*, *New Phytol.* **193**, 409 (2012).
11. H. Poorter, Ü. Niinemets, L. Poorter, I. J. Wright, R. Villar, *New Phytol.* **182**, 565 (2009).
12. I. J. Wright *et al.*, *New Phytol.* **166**, 485 (2005).
13. J. R. Evans, H. Poorter, *Plant Cell Environ.* **24**, 755 (2001).
14. M. E. McGroddy, T. Daufresne, L. O. Hedin, *Ecology* **85**, 2390 (2004).
15. P. B. Reich *et al.*, *Proc. R. Soc. London Ser. B* **277**, 877 (2010).
16. I. Aranda, F. Pardo, L. Gil, J. A. Pardos, *Acta Oecol.* **25**, 187 (2004).
17. T. Koike, M. Kitao, Y. Maruyama, S. Mori, T. T. Lei, *Tree Physiol.* **21**, 951 (2001).
18. U. Niinemets, J. D. Tenhunen, *Plant Cell Environ.* **20**, 845 (1997).
19. J. Kattge *et al.*, *Glob. Change Biol.* **17**, 2905 (2011).

Acknowledgments: The GLOPNET data set is archived in the online supplementary materials in (*2*) (DOI: 10.1038/nature02403) and is available at www.nature.com/nature/journal/v428/n6985/suppinfo/nature02403.html. J.L.D.O. and S.W.P. articulated the problem and analyses; J.L.D.O., J.W.L., and S.W.P. performed analyses; and J.L.D.O., S.W.P., J.W.L., and P.B.R. interpreted results and wrote the manuscript. P.B.R. thanks the NSF Long Term Ecological Research program (grant DEB 0620652) for support. No competing interests exist between the authors' funding sources and this research.

Supplementary Materials

www.sciencemag.org/cgi/content/full/science.1231574/DC1
Materials and Methods
Supplementary Text
Figs. S1 to S6
Tables S1 to S4
References (*20*–*22*)

16 October 2012; accepted 14 March 2013
Published online 28 March 2013;
10.1126/science.1231574

Early Mesodermal Cues Assign Avian Cardiac Pacemaker Fate Potential in a Tertiary Heart Field

Michael Bressan, Gary Liu, Takashi Mikawa*

Cardiac pacemaker cells autonomously generate electrical impulses that initiate and maintain the rhythmic contraction of the heart. Although the majority of heart cells are thought to originate from the primary and secondary heart fields, we found that chick pacemaker cells arise from a discrete region of mesoderm outside of these fields. Shortly after gastrulation, canonical Wnts promote the recruitment of mesodermal cells within this region into the pacemaker lineage. These findings suggest that cardiac pacemaker cells are physically segregated and molecularly programmed in a tertiary heart field prior to the onset of cardiac morphogenesis.

The rhythm of the heart is maintained by a specialized subclass of myocytes known as cardiac pacemaker cells (PCs). These cells generate action potentials (APs) in a cyclic manner to stimulate cardiac contractions. The anatomic position of mature PCs, the sinoatrial node (SAN), was described more than 100 years ago (*1*), however, little is known regarding the ontogeny or molecular mechanisms that specify PCs during development. This study was designed to address the timing, location, and mechanisms of PC cell fate acquisition.

Electrophysiological studies (*2*–*4*) have mapped cells that initiate cardiac APs to the inflow region at heart tube, looping, and septation stages. However, recent evidence indicates that as the heart matures, it continually expands, with cells being added to both the inflow and outflow segments

Cardiovascular Research Institute, University of California, San Francisco, CA 94143, USA.

*Corresponding author. E-mail: takashi.mikawa@ucsf.edu